VILNIUS UNIVERSITY

Life Science Center

2nd year student of Molecular Biology Master programme

Kristina JEVDOKIMENKO

Master Thesis

The Role of the Phospholipid Scramblase Xkr8 in the Developing Brain

Research supervisor:

Dr. Urtė Neniškytė, PhD

Vilnius, 2020

The Role of the Phospholipid Scramblase Xkr8 in the Developing Brain

Research was conducted at the Department of Neurobiology and Biophysics of the Institute of Biosciences of Life Sciences Center of Vilnius University.

Kristina Jevdokimenko   _____

Research supervisor

Allow / not allow to defend:

Dr. Urtė Neniškytė, PhD   _____

ACKNOWLEDGMENT

More than anyone else, I would like to thank my research supervisor **dr. Urtė Neniškytė**. I am beyond thankful for being trusted to be a part of an international project, to learn from the best specialist how to perform high quality research. Thank you for never ending motivation and encouragement for this project. I could not wish for a better supervisor for my work.

I would like to also thank dr. Urtė Neniškytė former and present group members at Life Sciences Center, Vilnius University: Simona, Ugnė, Dovydas, Viktorija, Kornelija, Daina, Arnas, Lina, Eimina, Gintarė, Avinash. Thank you for all the productive lab meetings and unconditional support.

I am also thankful to the Department of Neurobiology and Biophysics at Life Sciences Center and prof. Osvaldas Rukšėnas for helping me to start the research of Molecular Neuroscience.

I must thank my family who encouraged me and emotionally supported me at every step of my life. I will always be grateful to you.

I would like to thank my dearest friends: Aistė, Viktorija, Liutauras, Sigita, Kristina. Thank you for being there when I needed you the most.

CONTENTS

Abbreviations

a. u. – arbitrary units

act-casp-3 – active caspase-3

ANOVA – analysis of variances

cKO – conditional knock-out

DAPI – 4′,6-diamidino-2-phenylindole

Emx1 – empty spiracles homeobox 1

En – embryonic day n

GFP – green fluorescent protein

ICAM3 – intercellular adhesion molecule-3

IFB – infrapyramidal bundle

IQR – interquartile range

KO – knock-out

Ln – layer n

LSM – least squares means

MFG-E8 – milk fat globule-EGF factor 8

PBS – phosphate buffered saline

px – pixels

PFA – paraformaldehyde

Pn – postnatal day n

PtdSer – phosphatidylserine

S1 – primary somatosensory cortex

Thy1 – thymocyte differentiation antigen 1

vGlut1 – vesicular glutamate transporter 1

vGlut2 – vesicular glutamate transporter 2

WT – wild type

Xkr8 – XK-related protein 8

INTRODUCTION

During synaptic pruning synapses are eliminated from the neuronal network. This process needs to be strictly controlled, since under-pruning and over-pruning are associated with morphological and physiological impairments, leading to various neurodevelopmental diseases, such as autism spectrum disorder (Tang *et al.*, 2014) or schizophrenia (Glantz and Lewis, 2000).

It was thought, that synapse elimination is an autonomous neuronal process, but nowadays the amount of validated experiments is increasingly showing that during brain development synaptic pruning is mediated by brain macrophages – microglia (Paolicelli *et al.*, 2011).

There are numerous molecular signals in microglia-neuron interaction. They can be divided into two main groups: "eat-me" and "don't-eat-me" signals. "Eat-me" signals lead to phagocytosis and "don't-eat-me" signals prevent phagocytosis. One of the "eat-me" signals is phosphatidylserine (PtdSer), which gets exposed on the surface of the neuron and can then be recognised by vitronectin receptor expressed on microglia cells through a soluble PtdSer-specific opsonin milk fat globule-EGF factor 8 (MFG-E8) (Neniskyte and Brown, 2013). Therefore, synaptic pruning may be regulated by microglial phagocytosis of PtdSer-exposing neuronal structures.

Under normal conditions, most of PtdSer is maintained in the inner membrane of phospholipid bilayer of plasma membrane. PtdSer exposure on the cell surface is controlled by a group of proteins known as phospholipid scramblases. They non-specifically and bidirectionally transport PtdSer in the plasma membrane down its concentration gradient (Segawa and Nagata, 2015). One of PtdSer-exposing scramblases is active caspase-3-dependent XK-related protein 8 (Xkr8) (Suzuki, Imanishi and Nagata, 2016).

To understand how PtdSer exposure contributes to microglia-mediated synaptic pruning we investigated a transgenic $Xkr8^{Flx/Flx}$; $Emx1$::Cre; $Thy1$::GFP mouse line with impaired Xkr8 expression in Emx1 excitatory neurons. We were interested whether insufficient PtdSer exposure on Xkr8-lacking neurons will affect the elimination of the synapses of these neurons during brain development. For this purpose, we investigated two developmental time points (postnatal day 8, P8 – early neural network and postnatal day 28, P28 – juvenile neural network) of $Xkr8$ wild type ($Xkr8$-WT) and $Xkr8$ conditional knock out

(*Xkr8*-cKO) mice. We analysed two brain regions – cerebral cortex and thalamus. Cortical connections, expressing vesicular glutamate receptor 1 (vGlut1), expressed *Emx1* promoter, therefore were affected by Cre recombinase and lacked PtdSer scramblase Xkr8 in *Xkr8*-cKO animals. Thalamic connections, expressing vesicular glutamate receptor 2 (vGlut2), retained normal PtdSer scrambling in both *Xkr8*-WT and *Xkr8*-cKO mice due to the lack of Cre recombinase. Moreover, it is known that *Emx1*::Cre driver is expressed from the embryonic day 10.5 (E10.5), therefore we analysed whether conditional Xkr8 elimination affects cortical cell density. Finally, we analysed how disrupted PtdSer scrambling affects pruning of corticospinal axons.

The aim of this study was to investigate the role of Xkr8 scramblase-dependent PtdSer exposure in synaptic pruning.

Objectives

1. To assess the expression of Xkr8 scramblase in *Xkr8*-WT and *Xkr8*-cKO mice brain.
2. To evaluate synaptic pruning in developing somatosensory cortex and thalamus in *Xkr8*-WT and *Xkr8*-cKO mice.
3. To investigate the effect of conditional *Xkr8* knock-out on the developmental loss of cortical neurons.
4. To analyse the effect of disrupted PtdSer scrambling on corticospinal axonal pruning.

1. LITERATURE REVIEW

1.1 The role of synaptic pruning in brain development

Connections between two neurons are called synapses. During brain development the number of neuronal cells increases and more synapses are formed. Nevertheless, maturation of neural network is not defined by the increasing number of formed synapses. Neural network matures when excessive synapses are eliminated, whereas necessary synapses are sustained throughout the brain. This process, when synapses are removed, is called synaptic pruning.

During the maturation of neural network, synaptic loss, as a result of synaptic pruning, is observed in various parts of the brain. Synaptic pruning is required to get the monoinnervation of neuromuscular junction (Figure 1A-1, Smith *et al.*, 2013). Synaptic pruning is also needed for mossy fibers and Purkinje cells to form right connections in cerebellum (Figure 1A-2, Carrillo, Nishiyama and Nishiyama, 2013; Hashimoto and Kano, 2013).
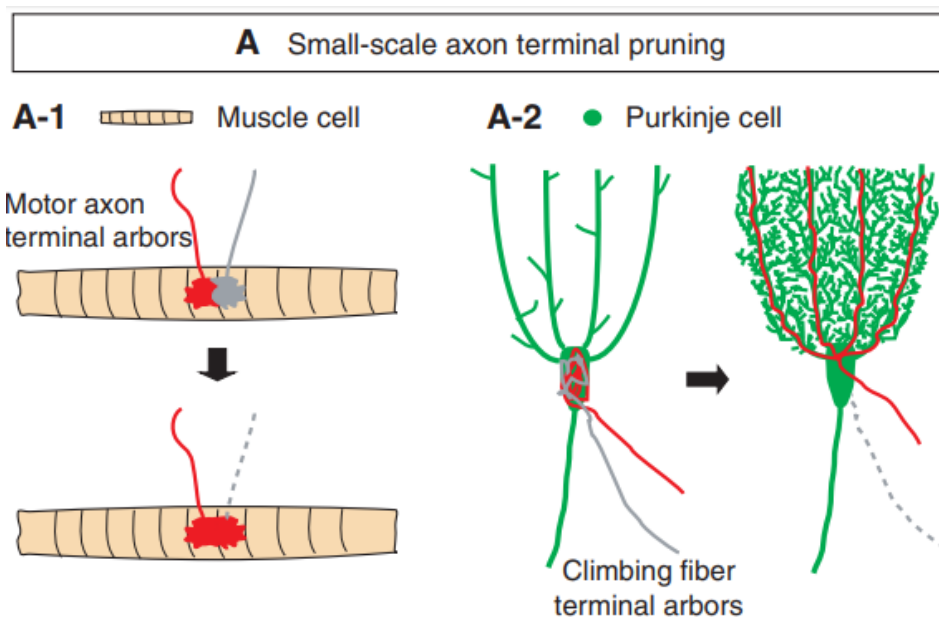
Figure 1. Small-scale axon terminal pruning. (**A-1**) During the development of the neuromuscular junction, multiple short axon terminal arbors compete for one muscle fiber, but only one arbor eventually stays. (**A-2**) During the development of the cerebellum, the cell body of a Purkinje cell is initially innervated by multiple climbing fiber terminal arbors, but later only one terminal arbor can make connections with the Purkinje cell, while all other terminal arbors are pruned (Vanderhaeghen and Cheng, 2009).

The process of synaptic pruning needs to be strictly controlled, since deviations from the optimal amount of neural connections can be associated with various neurodevelopmental disorders. When synaptic pruning is not active enough, too dense synaptic network may cause autism spectrum disorders (Tang *et al.*, 2014). The size of the brain of children with autism spectrum disorder significantly increases during the first year of development compared to neurotypical individuals. This might be caused by neuronal network that is too dense and too active microglia cells in the areas with too many synapses (Redcay and Courchesne, 2005; K. Suzuki *et al.*, 2013; Sacco, Gabriele and Persico, 2015).

The opposite condition, when neuronal network is too sparse due to over-active synaptic pruning, is observed in the brains of patients diagnosed with schizophrenia (Glantz and Lewis, 2000). First schizophrenia symptoms are noticed in later teenage years, when synaptic pruning in prefrontal cortex is almost finished (Selemon and Zecevic, 2015). Since schizophrenia is associated with decreasing volume of grey matter in prefrontal cortex, one of the reasons why schizophrenia occurs could be aberrant synaptic pruning.

1.2   Microglia – the macrophages of the brain

Brain is composed not only of neurons, but also of other types of cells. Besides neurons, which receive, process, and transmit neural impulses, there are abundant glial cells that perform important functions: astrocytes, oligodendrocytes and microglia cells. Astrocytes are the most frequent non-neuronal cells, which secure the transmission of neuronal signal by providing trophic support. Oligodendrocytes are responsible for the isolation of axons by myelin sheath in the central nervous system, while Schwann cells have this function in the peripheral nervous system. Finally, the brain has their own immune system, which is composed of brain macrophages – microglia (Aloisi, 2001). It is known, that microglia make up about 10% of brain cells, but they play a major role in brain development, neural network maturation and its maintenance, and brain injury.

Under normal circumstances, microglia cells are distributed all over the brain so that they are able to check every volume unit of the brain within couple of hours (Nimmerjahn, Kirchhoff and Helmchen, 2005). This way microglia cells scan the brain for injuries, cellular debris, and chemotactic signals (Casano and Peri, 2015).

Phagocytosis occurs in several steps – first of all, due to chemotaxis, microglia cells are attracted to phagocytic target. Signalling molecules on target cells can lead to phagocytosis ("eat-me" signals) or they can prevent phagocytosis ("don't eat me" signals). If

an "eat-me" signal is exposed on the surface of the cell, it can be recognised by microglia cells directly through phagocytic receptors or through soluble proteins known as opsonins (Brown and Neher, 2014).

While performing their function, microglia cells are affected by various signals, including chemokines. Chemokines are cytokines that induce chemotaxis of various cells (Sozzani *et al.*, 1996). One of the most researched brain chemokine is CX3C chemokine class member CX3CL1, also known as fractalkine. This protein is a signal molecule that directs microglia to excessive synapses (Liang *et al.*, 2009). Fractalkine is also exposed on the surface of neuronal cell where it may also act as a signal molecule to microglia cells. Fractalkine receptor CX3CR1, which recognises fractalkine, is only expressed on the surface of microglia (Mizutani *et al.*, 2012; Zhan *et al.*, 2014). Paolicelli *et al.* were the first to report that synaptic pruning by microglia is necessary for normal brain development. Researchers investigated fractalkine receptor knock-out mice (*Cx3cr1*-KO) and noticed significantly higher dendritic spine density of CA1 neurons in hippocampus. They also demonstrated that critical time period for microglia-mediated synaptic pruning was the second and the third postnatal weeks, since exactly then significantly higher dendritic spine density in *Cx3cr1*-KO mice pyramidal neurons was observed.

1.3 Molecular mechanisms of synaptic pruning

1.3.1 Complement system

Complement system is composed of a group of proteins and glycoproteins, essential for organism defence. Soluble complement components circulate in the blood and the extracellular matrix, while complement receptors reside in the plasma membranes of cells (Holers, 2014). Latest research shows, that at least in some areas of the brain synaptic pruning relies on the complement proteins that label synapses according to their activity (Schafer *et al.*, 2012; Holers, 2014; Presumey, Bialas and Carroll, 2017). In complement-dependent synaptic pruning more active synapses are pruned less than complement-marked less active synapses (Schafer *et al.*, 2012). Series of proteolytic reactions occur during this process, which results in a group of cleaved complement proteins, which then become the signals for microglia (Wyatt *et al.*, 2017). Neurons express complement component C1q, which causes the assembly of complement component 3 (C3) convertase, which then can cleave C3 into biologically active fragments C3a and C3b. C3a may cause inflammation, and it is known, that the aggregation of C3b, as well as C1q, on the surface of neuron is an "eat-me" signal for microglia, which has the complement receptor 3 (CR3) on its surface. Importantly, recent

studies show that C1q, C3 and CR3 are required for the synaptic pruning of the inputs of retinal ganglion cells in the dorsal lateral geniculate nucleus (Figure 5B-4). Here, complement system is required for bilateral vision formation (Stevens *et al.*, 2007; Schafer *et al.*, 2012; Stephan, Barres and Stevens, 2012).

1.3.2   "Eat-me" and "don't-eat-me" signals for microglia

There are numerous molecular signals in neuron-microglia interaction. They can be divided in to two main groups: "Eat-me" and "Don't-eat-me" (Figure 2, Brown and Neher, 2014). Once a "Don't-eat-me" signal is exposed on the surface of the cell it prevents phagocytosis, on the other hand "eat-me" signal induces phagocytosis.

"Eat-me" signals include some carbohydrates (mannose, Ogden *et al.*, 2001), intercellular adhesion molecule-3, (ICAM3, Kristóf *et al.*, 2013), calreticulin (Gardai *et al.*, 2005) and one of the most studied "eat-me" signals for microglia is a lipid molecule phosphatidylserine (PtdSer) (Nagata *et al.*, 2016) . Under normal conditions, most of PtdSer is maintained in the inner phospholipid leaflet of plasma membrane. PtdSer distribution between the inner and outer layers of plasma membrane is controlled by two protein groups. One of them are ATP-dependent flippases, directional phospholipid translocases, and the other – phospholipid scramblases, which transport phospholipids in a non-specific manner from the inner layer of phospholipid bilayer to the outer down their concentration gradient (Suzuki, Imanishi and Nagata, 2016). In order for PtdSer to be exposed on the surface of the cell, flippases need to be inhibited and scramblases have to be activated. PtdSer exposure can be triggered by activated, Ca^{2+}-dependent scramblase anoctamine-6 (ANO6, also known as transmembrane protein 16F, TMEM16F) and active caspase-3-dependent XK-related protein 8 (Xkr8) (J. Suzuki *et al.*, 2013; Suzuki, Imanishi and Nagata, 2014).
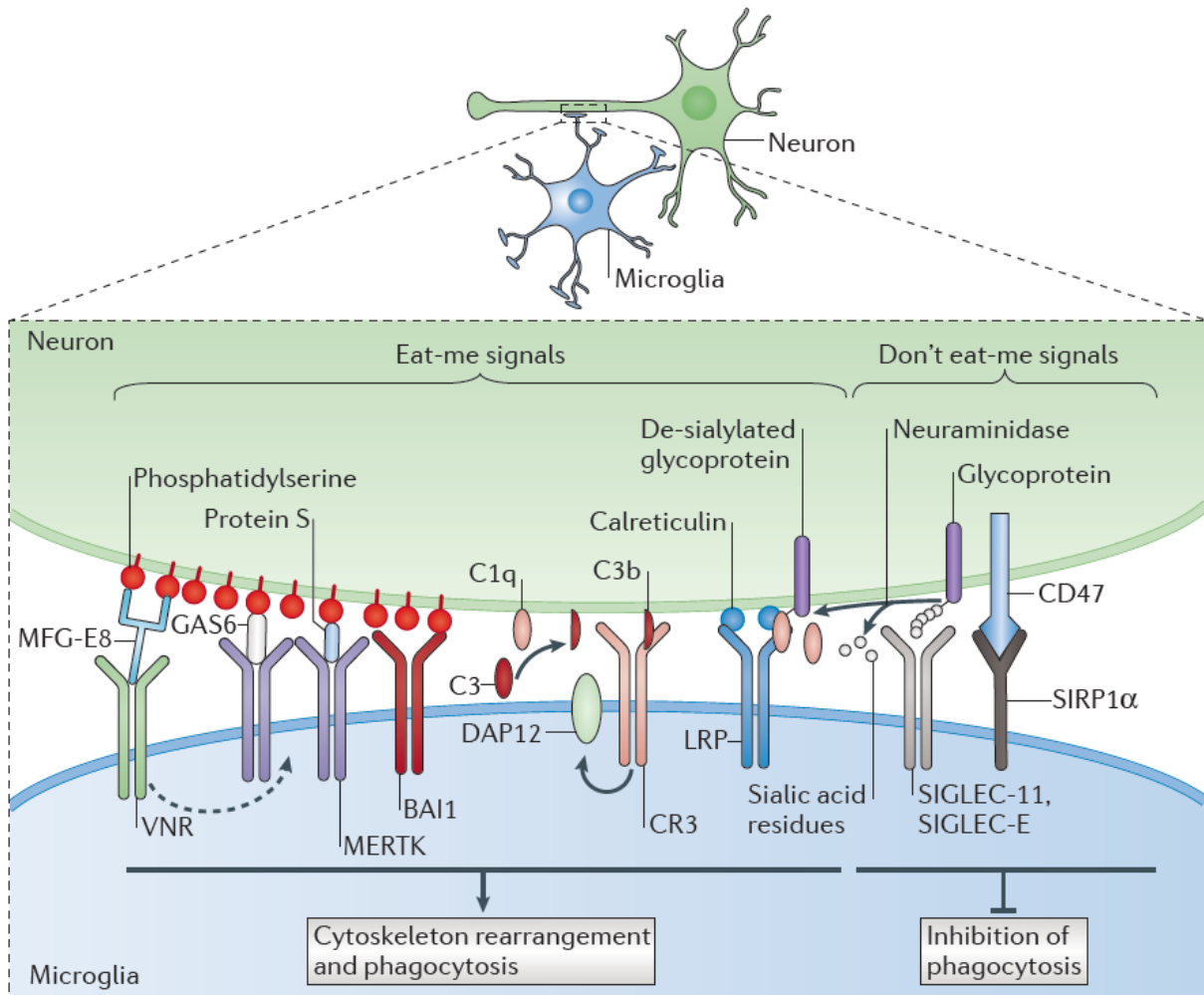
Figure 2. Signaling molecules in microglia-neuron interaction. "Eat-me" signals induce cytoskeleton rearrangement and phagocytosis and "Don't-eat-me" signals prevent phagocytosis. "Eat-me" signals can be recognised directly or through soluble proteins opsonins, which bind to microglia receptors. Phosphatidylserine can be recognised indirectly through milk fat globule-EGF factor 8 (MFG-E8). This in turn can induce phagocytosis by binding to vitronectin receptor (VNR). Dashed arrow depicts possible stimulation of MER receptor tyrosine kinase (MERTK) upon VNR activation. Complement component 1q (C1q) by binding to the surface of the neuron can activate complement component 3 (C3) cleavage to complement component 3b (C3b), which causes phagocytosis through microglial complement receptor 3 (CR3) (Brown and Neher, 2014).

PtdSer exposure on neuronal surface is known to be a phagocytic signal for microglia (Brown and Neher, 2014). Nevertheless, there is currently limited data on PtdSer exposure during brain development. Recent study has shown that ectopic PtdSer exposure on live neurons in *Drosophila* causes glial cells to engulf neurites in central nervous system (Sapar *et al.*, 2018). MER receptor tyrosine kinase (MERTK) and milk fat globule-EGF factor 8 (MFG-E8) specifically binds to PtdSer. Gene disruptions of *Mertk* (Chung *et al.*, 2013) in mice showed various synaptic pruning inaccuracy, thus suggesting that PtdSer may be a potential synaptic "eat-me" signal.

1.3.3   Xkr8 scramblase

One of the proteins, regulating PtdSer exposure on the surface of the cell, is Xkr8 scramblase (Suzuki, Imanishi and Nagata, 2014). During certain conditions, caspase-3 is activated in the cell, which in turn cleaves Xkr8 C-terminus, residing in the inner side of the membrane (J. Suzuki *et al.*, 2013; Suzuki, Imanishi and Nagata, 2014). This activates PtdSer transport from the inner to the outer phospholipid layer. Such regions of exposed PtdSer are then coated by soluble specific opsonins, such as MFG-E8, and can be recognised by a range of receptors (for example vitronectin receptor) on the surface of microglia (Figure 3) (Neniskyte and Brown, 2013).

Figure 3. The action mechanism of the Xkr8 scramblase. Active caspase-3 cleaves Xkr8 scramblase C-terminus thus activating it. Active Xkr8 can then transport phosphatidylserine (PtdSer) from the inner layer of the phospholipid membrane to the outer layer, where the regions of exposed PtdSer are coated by specific opsonin milk fat globule-EGF factor-8 (MFG-E8). "Eat-me" signal PtdSer is recognised through MFG-E8 by the vitronectin receptor expressed on the surface of the brain immune cells microglia (Adapted from Vadišiūtė, 2017).

1.4   Cortical connectivity

Cortical cell network is one of the most complex networks in the brain. Here, sensory information arrives from primary thalamus into all cortical layers, but most densely into layer IV (L4) and the layer V to VI (L5-L6) border (Figure 4, Harris and Mrsic-Flogel, 2013). L4 principal cells reside in a highly dense cortical layer IV and comprise two morphological classes, pyramidal and spiny stellate cells, whose intrinsic properties and coding strategies appear largely similar. L4 principal cells project to all layers, but most strongly to L2/3. They receive little intracolumnar input in return from primary thalamus.
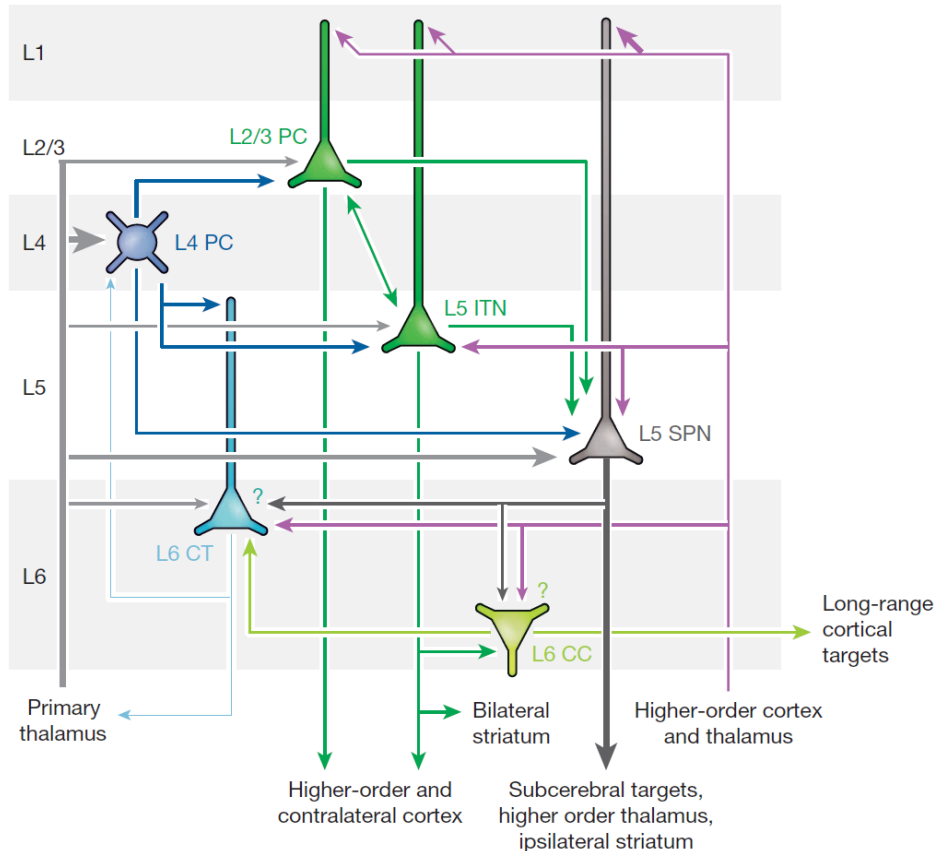
Figure 4. Connectivity of cortical cells. Primary thalamus projects to all cortical layers. L4 cells show strongest projection to L2/3 and a little effect on L4. L2/3 cells project to L5 locally or to higher-order and contralateral cortex. L5 intratelencephalic neurons (ITNs) project to L2/3 and distally to the ipsi- and contralateral cortex and striatum. L1 are mainly receiving inputs from subcerebral projection neurons (SPNs), which exhibit inverse connectivity pattern to L4 principal cells. SPNs project to subcerebral motor centres, and can directly drive movements. Their axons send collaterals to ipsilateral striatum and higher-order thalamus (Harris and Mrsic-Flogel, 2013).

1.5   Developmental axonal pruning

There have been identified several large-scale stereotyped axon pruning systems. First shown ever was the remodeling of cortical callosal axon branches that project to the contralateral side of the brain in the cerebral cortex (Figure 5B-1, Innocenti and Price, 2005).

Other large-scale stereotyped axonal pruning in the cerebral cortex is the refinement of subcortical axons of visual and motor cortices (Figure 5B-2). Axons originating from neurons of these two cortices initially project to subcortical targets that overlap in the brain stem and spinal cord. Later in development, only the functionally appropriate collateral branches for each cortical region are maintained. Therefore, neurons from the visual cortex prune away their branches that extend to motor system targets. On the other hand, neurons

from the motor cortex prune their branches that extend to the visual superior colliculus. The axon collaterals are removed within the first few weeks of postnatal development.

The hippocampus is another area in the CNS which demonstrates considerable remodeling of projections (Bagri *et al.*, 2003). During development, granule cells of the dentate gyrus project two bundles of mossy fiber axons to CA3: a main bundle that courses adjacent to the apical dendrites of CA3 pyramidal cells, and a transient infrapyramidal bundle (IFB) of axon collaterals that course adjacent to the basal dendrites of the pyramidal cells (Bagri *et al.*, 2003). The transient long IPB is stereotypically pruned back later in development.
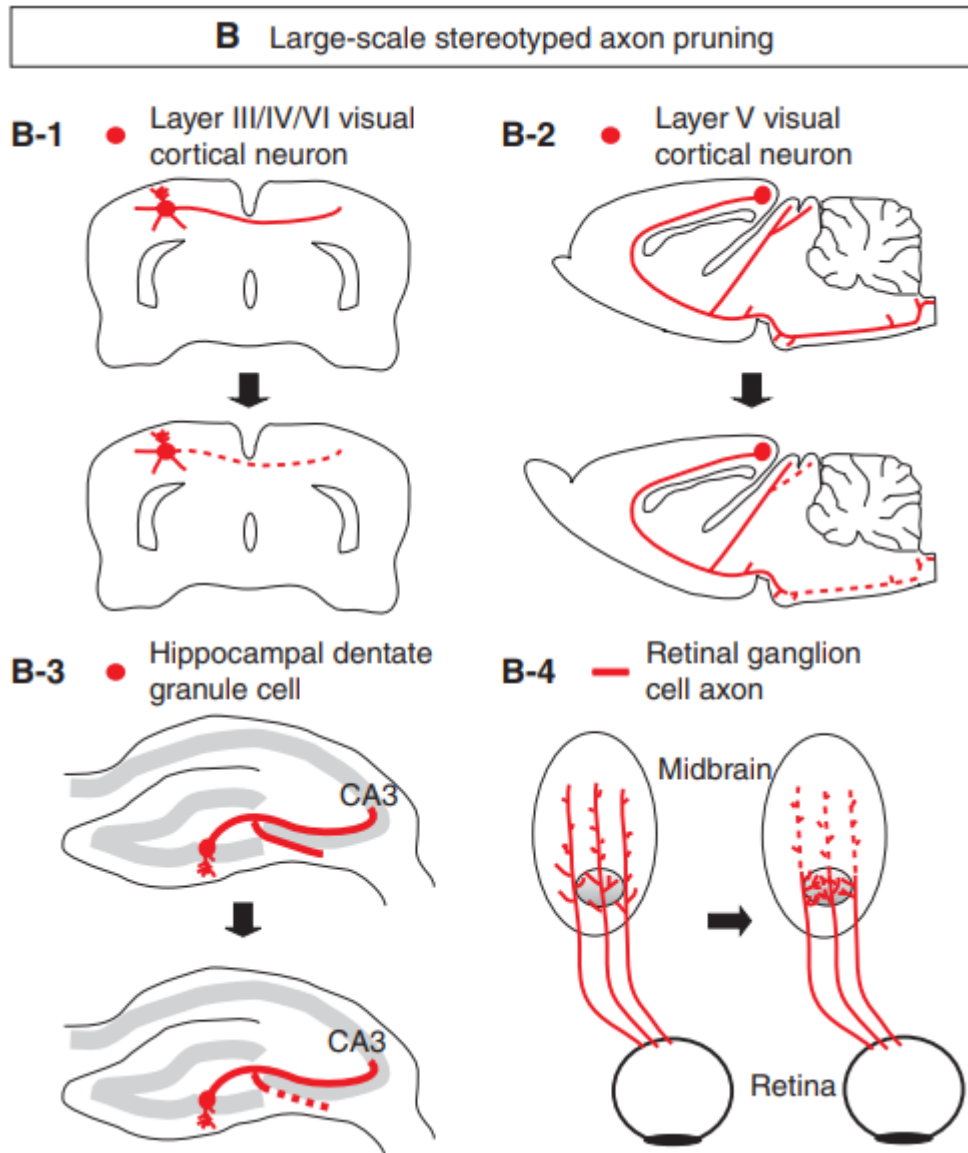
Figure 5. Large-scale stereotyped axon pruning. (**B-1**) During the development of the visual cortex, long projections from L3/4/6 visual cortical neurons to the contralateral cortex are pruned. (**B-2**) During the development of corticospinal projections, long projections of L5 visual cortical neurons to multiple subcortical target regions are pruned. (**B-3**) During the pruning of hippocampal mossy fibers, the infrapyramidal branches of the mossy fibers from the dentate granule cells to the CA3 region are pruned. (**B-4**) During the development of the retinal ganglia, the overextended retinal axons that pass their terminal zone in the midbrain are pruned (Vanderhaeghen and Cheng, 2009).

2. MATERIALS AND METHODS

2.1 MATERIALS

The following tables list materials, equipment and software used in this thesis.

2.1.1 Reagents

Chemicals and reagents	Manufacturer
DAPI (4′,6-diamidino-2-phenylindole)	Invitrogen
di-Sodium tetraborate anhydrous	Roth
F-type immersion	Leica
Gold (III) chloride	Sigma-Aldrich
Hydroquinone	Roth
Mowiol	Calbiochem
Nitric acid	Roth
Normal goat serum	Invitrogen
Oxalic acid dihydrate	Roth
Paraformaldehyde	Sigma-Aldrich
PBS	Invitrogen
Silver nitrate	Roth
Sodium azide	Merck
Sodium sulphite anhydrous	Roth
Sodium thiosulphate pentahydrate	Roth

2.1.2 Consumables

Consumable	Manufacturer
24-well plates	Costar
48-well plates	Costar
Coverslips (60 × 24 mm) #1	Roth
Microscope slides (76 × 26 mm)	Roth
Superfrost Plus™ Adhesion Microscope Slides	ThermoFisher Scientific

2.1.3 Antibodies

Primary antibodies

Primary antibody	Manufacturer
Mouse anti-vGlut2	Abcam
Rabbit anti-vGlut1	Synaptic Systems
Rabbit anti-Xkr8	Rockland

Secondary antibodies

Secondary antibody	Manufacturer
Goat anti-mouse-Alexa Fluor®568	Invitrogen
Goat anti-rabbit-Alexa Fluor®647	Invitrogen

2.1.4   Equipment and software

Equipment and software	Manufacturer / Reference
TCS SP5 resonant scanner	Leica
TCS SP8 resonant scanner	Leica
OLYMPUS PROVIS AX70 microscope	OLYMPUS
LAS AF	Leica
LAS X	Leica
Image-Pro Plus 6.1	Media Cybernetics, Inc.
ImageJ 2.0.0-rc-65/1.51w	National Institutes of Health (NIH)
Excel	Microsoft, Inc.
STATISTICA 13.3	TIBCO Software Inc.
GraphPad Prism v6.00	GraphPad Software (La Jolla, California, USA)

2.2   METHODS

2.2.1   Animals

Transgenic mice lines used in this study are described in Table 1.

Table 1. Genotypes of animal lines used in this study.

Genotype	Description	Reference
Thy1::GFP	Transgenic mouse line, where green fluorescent protein (GFP) is expressed under the control of *Thy1* promoter for neuronal expression. *Thy1*::GFP mice express GFP in subset of motor axons, retina ganglion cells, mossy fibers, and cortex neurons. *Thy1* expression is the highest in developing neurons.	(Kemshead *et al.*, 1982; Feng *et al.*, 2000)
Xkr8$^{Flx/Flx}$	*Xkr8* conditionally targeted mice were developed using neo-loxP cassette system. 1.0 kb fragment containing exon 3 was replaced with a sequence that flanked *Xkr8* gene locus by loxP sequence. LoxP sites were inserted upstream and downstream of *Xkr8* gene.	(J. Suzuki *et al.*, 2013)
Emx1::Cre	This mouse line expresses Cre recombinase in the endogenous *Emx1* locus. *Emx1* is expressed in developing neurons. When crossed with a line containing loxP sites, Cre-mediated recombination ensures the deletion of flanked sequence. Recombination occurs in majority of neocortical and hippocampal neurons. *Emx1* is expressed in a subset of male germline cells.	(Iwasato *et al.*, 2000, 2004)

2.2.2   Brain sectioning

Brains from P8, P28 *Xkr8*$^{Flx/Flx}$; *Emx1*::WT; *Thy1*::GFP (wild type, WT) and P8, P28 *Xkr8*$^{Flx/Flx}$; *Emx1*::Cre; *Thy1*::GFP (conditional knock out, cKO) mice (3 animals per experimental group) were fixed by perfusion and then post-fixed in 4% paraformaldehyde overnight at 4°C. Coronal sections of anterior brain (50 µm in thickness) and medulla (30 µm in thickness) were cut with vibratome and stored in 24-well plates containing 0.02% sodium azide in PBS. (Animal perfusion was performed by Matteo Gaettani at the European Molecular Biology Laboratory, Italy.)

2.2.3   Immunohistochemical staining

Brain sections were permeabilized in 0.4% Triton X-100 with 20% normal goat serum in PBS for 2 h at room temperature. Then, they were incubated with primary antibodies in 0.4% Triton X-100 and 20% normal goat serum in PBS overnight at 4°C. For the assessment of Xkr8 expression primary antibodies were used against Xkr8 protein and for the evaluation of synaptic pruning in developing somatosensory cortex and thalamus – against vGlut1 (vesicular glutamate transporter 1) and vGlut2 (vesicular glutamate transporter 2).

After that, the sections were washed three times for 15 min with PBS and incubated with secondary antibodies in 5% normal goat serum in PBS for 2 hours at room temperature. Secondary antibodies were conjugated to fluorophores AlexaFluor568 (Xkr8 or vGlut2) and AlexaFluor647 (vGlut1). Sections were then washed again three times for 15 min with PBS and incubated with DAPI (4′,6-diamidino-2-phenylindole, which intercalates in nucleus residing DNA) for 15 min (final dilution 1:1000), and washed three times for 15 min with PBS. Primary and secondary antibodies used for immunohistochemical stainings are described in Table 2.

Table 2. Primary and secondary antibodies used for immunohistochemical stainings.

Binding specificity	Host	Dilution	Blocking serum
Anti-Xkr8	Rabbit	1:100	Goat
Anti-vGlut1	Rabbit	1:500	Goat
Anti-vGlut2	Mouse	1:500	Goat
Anti-rabbit-AF647	Goat	1:500	Goat
Anti-mouse-AF568	Goat	1:500	Goat

Stained brain sections were placed on microscope slides, air dried and mounted with Mowiol. The mounting medium was hardened overnight at room temperature, afterwards slides were stored at 4°C in the dark. The preparation of experimental animals and the immunohistochemistry for vGlut1 and vGlut2 was performed by Augustė Vadišiūtė and dr. Urtė Neniškytė.

2.2.4 Modified Palmgren silver staining

We used modified Palmgren silver staining described by (Goshgarian, 1977) to visualise corticospinal tracts in P8 and P28 *Xkr8*-WT and *Xkr8*-cKO mice. Medulla sections were placed on the adhesion microscope slides, air dried and dehydrated through graded 70 % to absolute ethanol and rehydrated back to distilled water for uniform staining. For better impregnation of terminal axon arbours, sections were treated with 0.15 M 2-amino-2-methyl-1-propanol solution (adjusted with nitric acid to 5.0 pH) for 7 min and washed in three changes of distilled water, each 1.5 min. Then sections were impregnated in 10 % aqueous silver nitrate for 45 min at 37°C. After impregnation, sections were transferred without rinsing to freshly prepared 2 % sodium borate for 10 s, agitated and rinsed in distilled water until the precipitate was removed. Then sections were developed in 2 % fresh sodium borate solution containing 0.05 % hydroquinone and 5 % sodium sulphite for 15 min at 37°C and rinsed three times in 50 % ethanol, each 1.5 min. Then sections were toned with 0.5 % gold

chloride solution for 5 min and rinsed with distilled water. After that, the staining was intensified with 0.5 % oxalic acid in 50 % ethanol for 2 min at 37°C and rinsed in distilled water. Finally, sections were fixed in 5 % sodium thiosulphate for 20 s, rinsed, dried, cleared, mounted with Mowiol and left to harden overnight at room temperature. The slides were stored at 4°C until imaging.

2.2.5   Imaging

Leica SP8 resonant scanner confocal microscope with 63× 1.4NA immersion objective was used to image S1 area of somatosensory cortex, hippocampus and nucleus reuniens of thalamus (3.9 zoom, pixel size 46×46 nm^2). Two images of full length primary somatosensory cortices (200 µm width), both hippocampi and one image of thalamus were acquired per brain slice in *Xkr8*-WT and *Xkr8*-cKO mice. Fluorophores were excited using white light laser (excitation wavelength 568 nm – Xkr8).

Leica SP5 resonant scanner confocal microscope with 63× 1.4NA immersion objective was used to image S1 area of somatosensory cortex and nucleus reuniens of thalamus (5.2 zoom, pixel size 46×46 nm^2, z-axial step size 118 nm). Stacks of 10 imaging planes each were acquired for 30 fields of view per animal. Fluorophores were excited using DPSS laser (excitation wavelength 561 nm – vGlut2) and HeNe laser (excitation wavelength 633 nm – vGlut1).

Leica SP8 resonant scanner confocal microscope with 20× 0.75NA air objective and LAS X Navigator was used to image S1 area of somatosensory cortex to acquire DAPI-stained images. Two images (200 µm width) of full length primary somatosensory cortices were acquired per brain slice (2-8 images per animal). DAPI was excited using UV Diode (excitation wavelength 405 nm). LAS X Mosaic Merge tool (Type: Smooth) was used to merge tile scans.

OLYMPUS bright field microscope with 60× 1.25NA oil objective and Image-Pro Plus 6.1 software was used to image silver-stained corticospinal tracts in medulla sections. Three to four images (1280×1024 px, pixel size 75×75 nm^2) containing randomly selected axon bundles were acquired per brain slice (30 images per animal).

All obtained images then were subjected for image analysis.

2.2.6 Image analysis

Confocal images were analysed using open source image analysis software Fiji (ImageJ, NIH).

To count and compare DAPI-stained nuclei in layer IV and whole primary somatosensory cortex in P8 and P28 *Xkr8*-WT and *Xkr8*-cKO mice, the images were first pre-processed using Enhance Contrast (saturated value set to 0.35 for all images), Despeckle function to reduce noise, Mean filter (radius = 2), Kuwahara filter (sampling = 7) and Gaussian Blur (sigma = 2). Then threshold (Method – Otsu) was manually adjusted and a binary mask was created. Then Watershed operation was applied to separate all merged objects and resulting regions of interest were counted using Analyze Partices function (size = 10-Infinity). Then layer IV was manually cropped from all images and analysed as described above. In addition, area of both primary somatosensory cortex and layer IV was measured using Measure function. This analysis resulted in number of cortical cells, thickness of the cortex (μm), cortical cell density (cortex cells / μm^2), number of layer IV cells, thickness of the layer IV and layer IV cell density (layer IV cells / μm^2).

To count and compare the density of cortico-cortical and thalamo-cortical connections in primary somatosensory cortex and thalamocortical and intrathalamic connections in *Xkr8*-WT and *Xkr8*-cKO mice, both vGlut1 and vGlut2 confocal image stacks were analysed using same parameters. First of all, Z projection (projection type: Max Intensity) was performed, background was subtracted (rolling ball radius: 50 px) and Gaussian blur filter ($\sigma = 2$) was applied to all images. Then, "Find Maxima" (output type: Maxima Within Tolerance) operation was performed, with noise tolerance set as 10 to all images. Resulting image showed analysed signal as puncta and was counted using "Analyze Particles" function (size: 0-infinity, circularity: 0.00-1.00). The workflow of this analysis is shown in Figure 6 and was automated using macros function in ImageJ software (Figure 7).
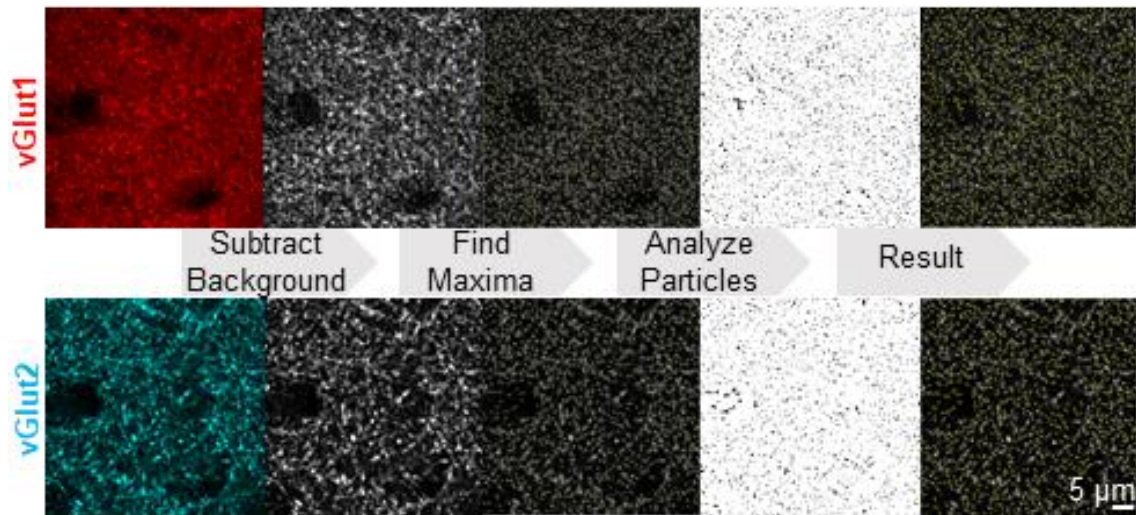
Figure 6. vGlut1 (red) and vGlut2 (cyan) image analysis workflow using ImageJ software (NIH).

```
run("8-bit")
run("Z Project...", "start=1 stop=10 projection=[Max
Intensity]");
run("Subtract Background...", "rolling=50");
run("Gaussian Blur...", "sigma=2");
run("Find Maxima...", "noise=10 output=[Maxima Within
Tolerance]");
run("Analyze Particles...", "summarize");
```

Figure 7. The macro used for vGlut1 and vGlut2 image analysis in ImageJ software (NIH).

To analyse normal and impaired PtdSer scrambling in cortical and thalamic connections in primary somatosensory cortex and thalamus, constant stack size (10 planes) was set for all images during confocal imaging. To precisely evaluate vGlut1+ cortical connections and vGlut2+ thalamic connections, analysed signals were counted in the field of view. Then they were normalised by constant image area (2243 μm^2) to obtain vGlut1 or vGlut2 density. To evaluate the ratio of vGlut1 to vGlut2, number of vGlut1 puncta was divided by number of vGlut2 puncta in the same field of view.

To count and compare silver-stained corticospinal cross-sections in medulla sections in P8 *Xkr8*-WT and *Xkr8*-cKO mice, the images were first pre-processed using Enhance Contrast (saturated value set to 0.35 for all images). Then axon-containing bundle was manually cropped from the image. After this, Mean filter (radius = 2) was applied and Find Maxima (Prevalence > 3-10, Output type = Maxima Within Tolerance) function was used to

identify individual axons. Resulting regions of interest were counted using Analyze Particles function (size = 0-Infinity) and number of cross-sections of corticospinal axons was obtained.

2.2.7   Statistics

All data is shown as mean ± SEM, scatter plot represents individual animals and was analysed using either STATISTICA 13.3, Excel MS or GraphPad Prism v6.0. Outliers were identified as exceeding median ± 3IQR, and were removed from following analyses. Mixed model analysis of variances (ANOVA) followed by least squares means (LSM) *post hoc* test was used to evaluate changes between genotypes during different days of postnatal development. Random effect of variance of mice was included into ANOVA model. Mann-Whitney test was used to evaluate changes between genotypes in corticospinal tract analysis. Threshold for significance levels was set at 0.05 ($p > 0.05$ – not significant, $0.01 < *p < 0.05$ – significant, $0.001 < **p < 0.01$ – very significant, $***p < 0.001$ – highly significant).
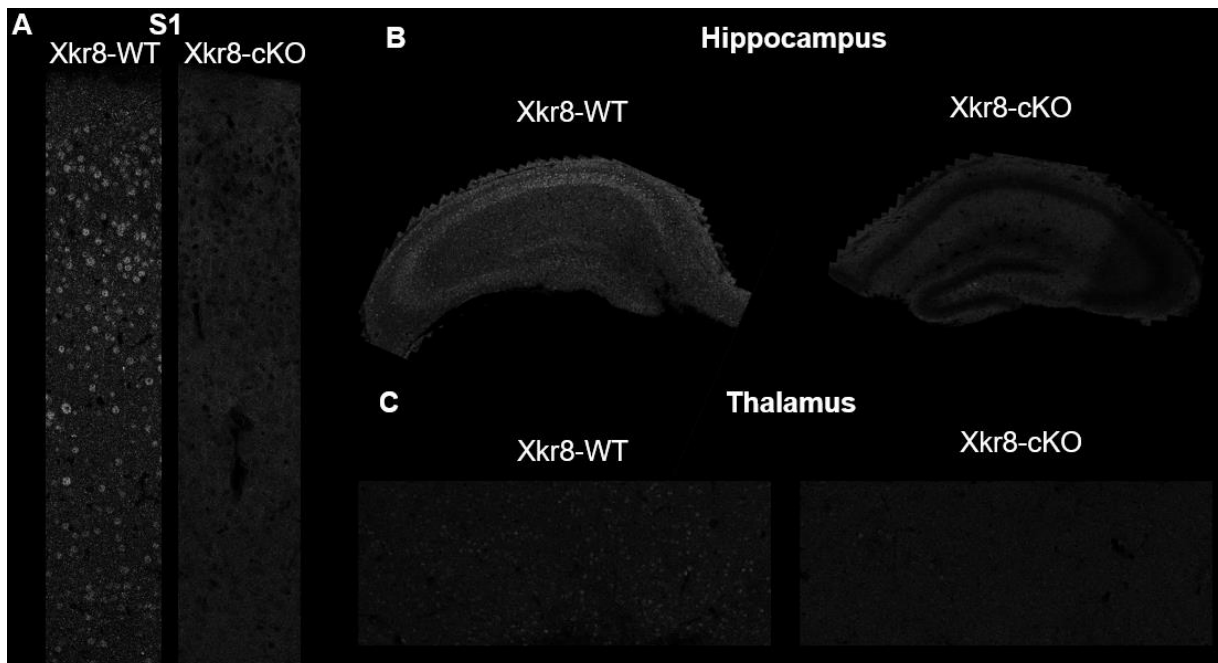
3. RESULTS

In this study, we investigated the role of phosphatidylserine scramblase Xkr8 in brain development. To understand how PtdSer exposure contributes to microglia-mediated synaptic pruning we investigated a transgenic *Xkr8*$^{\text{Flx/Flx}}$; *Emx1*::Cre; *Thy1*::GFP mouse line with impaired Xkr8 expression in Emx1 excitatory neurons. We were interested whether insufficient PtdSer exposure on Xkr8-lacking neurons will affect the elimination of the synapses of these neurons during brain development. For this reason, we investigated two sets of connections differing in PtdSer exposure. In cortex, we assessed cortico-cortical and thalamo-cortical connections. In thalamus, we analysed cortico-thalamic connections and thalamo-thalamic connections. It is known that *Emx1*::Cre driver expressed in our *Xkr8*-cKO mice line and is active during major events in cortical neurogenesis, such as postnatal cortical cell loss. Therefore, we investigated whether ablation of Xkr8 scramblase in excitatory neocortical neurons affected their development. Finally, we used a well described corticospinal tract system to evaluate cortical axonal pruning under normal and impaired Xkr8 scramblase expression.

3.1 Xkr8 is eliminated from the neocortical neurons in *Xkr8*-cKO mice

To evaluate Xkr8 expression on protein level we performed immunohistochemical staining against Xkr8 scramblase in *Xkr8*-WT mice (Figure 8). Xkr8 scramblase was found in the primary somatosensory cortex (Figure 8A, *Xkr8*-WT) and in the granular cell layer of hippocampus (Figure 8B, *Xkr8*-WT). To complement this data, we used RNAscope to evaluate *Xkr8* exon 3 gene expression in *Xkr8*-WT mice and found that the expression locations were similar (Supplementary Fig. 1).

To assess the impact of PtdSer scrambling in synaptic pruning we generated conditional *Xkr8* knock out mice line using Cre-loxP system, targeting *Xkr8* exon 3 (Table 1). Immunohistochemical staining against Xkr8 scramblase showed that there was no specific signal in either primary somatosensory cortex (S1) or hippocampus in *Xkr8*-cKO mice (Figure 8A-B, *Xkr8*-cKO), thus indicating that *Xkr8* was specifically eliminated from pyramidal neurons of the neocortex. Interestingly, we noticed lower Xkr8 expression in thalamus in *Xkr8*-cKO mice, where *Emx1* promoter was not expressed, therefore Xkr8 scramblase was maintained. This might have indicated that baseline expression of Xkr8 in thalamus is lower than in cortex. Moreover, cells residing in this region might have been mostly receiving cortical inputs, thus showed low Xkr8-specific signal, when Xkr8 was eliminated in *Xkr8*-cKO mice.

Figure 8. Immunohistochemical staining against Xkr8 scramblase in P8 *Xkr8*-WT and P8 *Xkr8*-cKO mice. Qualitative images of Xkr8 signal (white) in (**A**) primary somatosensory cortex (S1), (**B**) hippocampus and (**C**) thalamus in P8 *Xkr8*-WT and P8 *Xkr8*-cKO mice.

3.2 Synaptic pruning in developing somatosensory cortex and thalamus in *Xkr8*-WT and *Xkr8*-cKO mice

To understand how PtdSer exposure contributes to microglia-mediated synaptic pruning we investigated the synaptic density of neurons with impaired PtdSer scrambling. We were interested whether PtdSer-exposure in presynaptic or postsynaptic compartment is required for the removal of synaptic connections during brain development. For this purpose, we investigated *Xkr8*-WT and *Xkr8*-cKO mice at two developmental time points (postnatal day 8, P8 – premature neural network and postnatal day 28, P28 – juvenile neural network). We compared cortical connections, which expressed *Emx1* promoter (Iwasato *et al.*, 2004), therefore were affected by Cre recombinase and lacked PtdSer scramblase Xkr8 in *Xkr8*-cKO mice and thalamic connections, which maintained normal PtdSer scrambling in both *Xkr8*-WT and *Xkr8*-cKO animals (Figure 9A, B). Cortical pre-synapses were identified by specific expression of vesicular glutamate transporter 1, while thalamic pre-synapses were identified by vesicular glutamate transporter 2 (Fremeau Jr *et al.*, 2004, Figure 9C, D). Two sets of connections were investigated in each region. In cortex, we investigated cortico-cortical and thalamo-cortical connections (Figure 9B, C). In thalamus, we analysed cortico-thalamic connections and thalamo-thalamic connections (Figure 9B, D).
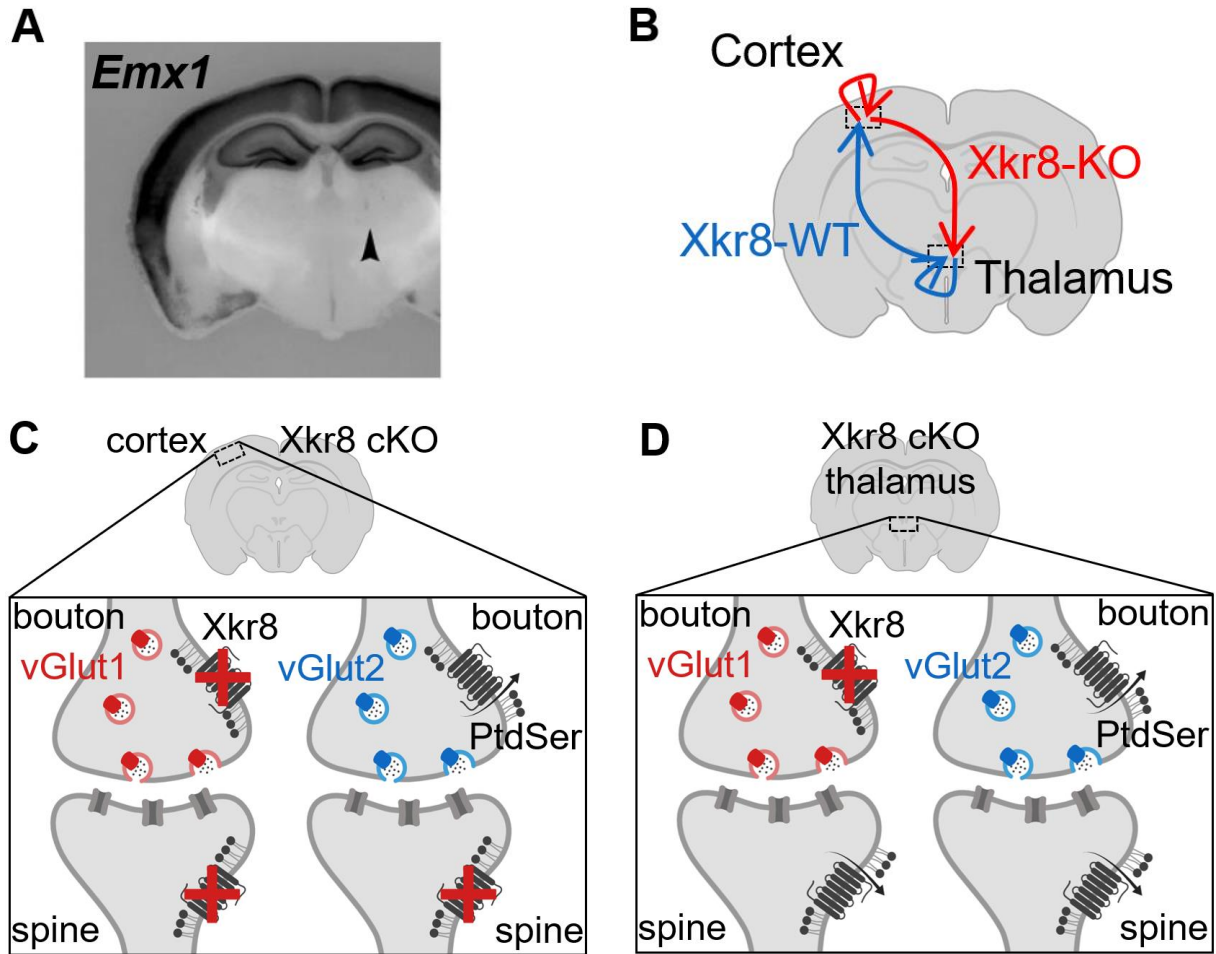
Figure 9. Experimental approach for investigation of the role of presynaptic PtdSer-exposure in synaptic pruning during brain development. (**A**) Representative image of *Emx1* (black) expression (Iwasato *et al.*, 2004). (**B**) Schematic diagram depicting the projections of *Xkr8*-WT neurons (blue arrows) and *Xkr8*-KO neurons (red arrows) in the regions of cortex and thalamus. (**C**) PtdSer exposure in cortex of *Xkr8*-cKO animals with impaired PtdSer scrambling in presynaptic vGlut1+ compartment and postsynaptic compartment, whereas presynaptic vGlut2+ compartment maintains normal PtdSer exposure. (**D**) PtdSer scrambling in thalamus of *Xkr8*-cKO animals with impaired PtdSer scrambling in presynaptic vGlut1+ compartment of corticothalamic synapse, meanwhile none of the thalamic synapses was affected.

3.2.1 Disrupted Xkr8 expression causes aberrant synaptic densities in mouse cortex

To find what impact PtdSer exposure in presynaptic compartment has in synaptic pruning during brain development, we investigated cortico-cortical and thalamo-cortical connections in primary somatosensory cortex of *Xkr8*-WT and *Xkr8*-KO mice at P8 and P28 time-points of development. *Xkr8*-WT experimental group had normal Xkr8 activity in both cortico-cortical and thalamo-cortical connections, meaning PtdSer was exposed normally in both presynaptic and postsynaptic compartments. In *Xkr8*-cKO brains scramblase was eliminated from cortical connections, therefore PtdSer was only exposed normally in presynaptic compartment of thalamo-cortical connections, whereas both presynaptic and postsynaptic PtdSer scrambling was impaired in cortico-cortical connections (Figure 9).

In developing *Xkr8*-WT brain, we observed significant increase of vGlut1 and vGlut2 (p<0.001) from P8 to P28 (Figure 10A, B). There was no significant difference in vGlut1 and vGlut2 ratio between P8 and P28 in *Xkr8*-WT mice (Figure 10C). This showed that in the primary somatosensory cortex the density of both cortico-cortical and thalamo-cortical connections increases during brain development and their ratio is stable.

Impairment of PtdSer exposure caused three-fold increase of vGlut1 puncta at P8 in *Xkr8*-KO mice (p<0.001, Figure 10A). In contrast, there was no significant increase of vGlut2 puncta in P8 *Xkr8*-KO mice, indicating that aberrant synaptic density was restricted to pyramidal cortical neurons (Figure 10B, E). There was also no significant difference in vGlut1 and vGlut2 ratio between P8 and P28 *Xkr8*-cKO mice (Figure 10F). This suggested that corticocortical and thalamocortical connections balance one another out during cortical development. In comparison to *Xkr8*-WT mice, ratio increased twice both in premature (p<0.001) and mature (p<0.001) primary somatosensory cortex (Figure 10F). This confirmed higher density of vGlut1+ puncta (Figure 10B, D). We concluded that synaptic pruning of connections with impaired PtdSer exposure in presynaptic compartment were affected, whereas PtdSer exposure impairment in postsynaptic compartment did not affect pruning.
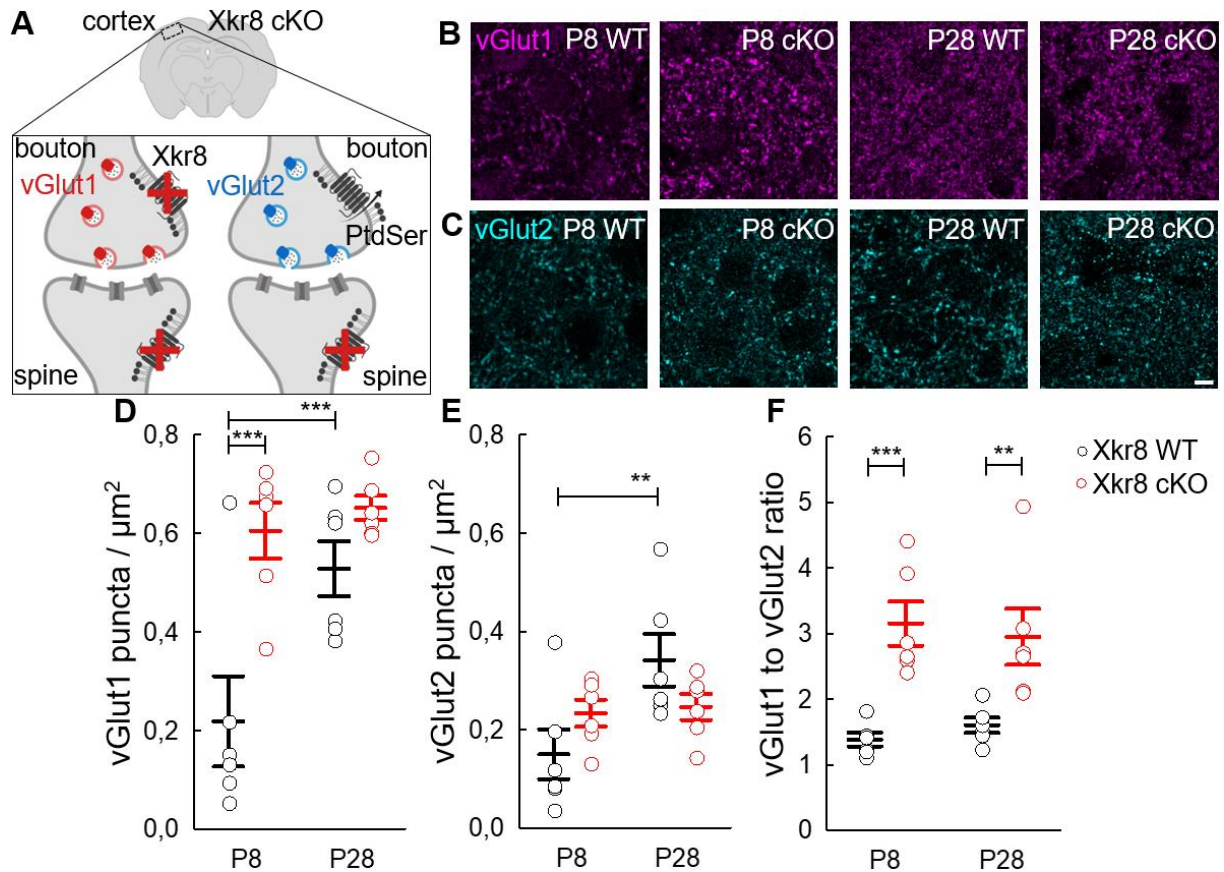
Figure 10. Synapse density in developing cortex of *Xkr8*-WT and *Xkr8*-cKO mice. (**A**) Schematic representation of PtdSer exposure in *Xkr8*-cKO cortex. Representative images of (**B**) vGlut1+ and (**C**) vGlut2+ puncta in P8 *Xkr8*-WT, P8 *Xkr8*-cKO, P28 *Xkr8*-WT, P28 *Xkr8*-cKO hippocampus (scale bar 5 μm). The density of (**D**) vGlut1+ and (**E**) vGlut2+ puncta / μm^2 and (**F**) the ratio of vGlut1+ to vGlut2+ in cortex in developing *Xkr8*-WT and *Xkr8*-cKO mice cortex. All data shown as mean ± SEM, scatter plot represents individual animals, n = 6. Mixed model ANOVA, LSM *post-hoc* test, ***p<0.001.

### 3.2.2 Impaired PtdSer exposure in presynaptic compartment disrupts synaptic pruning in thalamus

We then investigated how PtdSer exposure affects pruning in thalamus, where Xkr8 scramblase was only knocked-out from incoming cortical connections (Figure 11A).

We observed a significant increase (p<0.01) in the densities of vGlut1+, but not vGlut2+ puncta when comparing P8 and P28 *Xkr8*-WT mice (Figure 11B-E). The ratio of vGlut1+ to vGlut2+ also increased (p<0.05) from P8 to P28 in *Xkr8*-WT mice (Figure 11F). This showed that during brain development the density of incoming cortico-thalamic synapses increased in the neuronal network of thalamus.

Interestingly, the conditional knock-out of Xkr8 scramblase caused significant increase in the densities of vGlut1+ (p<0.001) and vGlut2+ (p<0.01) puncta in P8 *Xkr8*-cKO

mice, but the ratio of vGlut1+ to vGlut2+ was not altered when comparing *Xkr8*-WT and *Xkr8*-cKO mice (Figure 11B-F). This might indicate that corticocortical and thalamocortical connections maintained balance to one another when Xkr8 expression was impaired in incoming corticothalamic axons. Overall, the impairment of PtdSer scrambling in presynaptic compartment disrupted synaptic pruning, whereas postsynaptic PtdSer was not sufficient to trigger and/or mediate synaptic pruning.
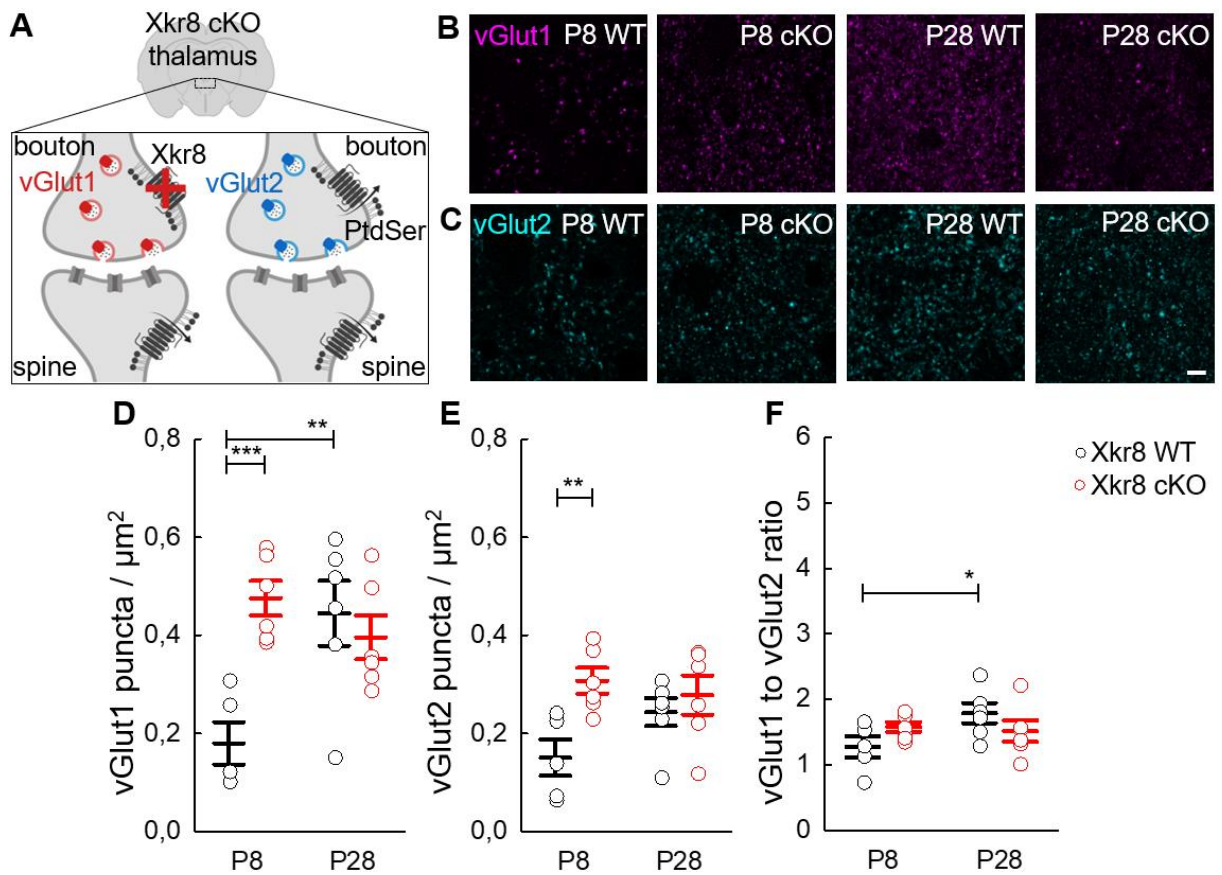

Figure 11. Synapse density in developing nucleus reuniens of *Xkr8*-WT and *Xkr8*-cKO mice. (**A**) Schematic representation PtdSer exposure in *Xkr8*-cKO thalamus. Representative images of (**B**) vGlut1+ and (**C**) vGlut2+ puncta in P8 *Xkr8*-WT, P8 *Xkr8*-cKO, P28 *Xkr8*-WT, P28 *Xkr8*-cKO thalamus (scale bar 5 µm). The density of (**D**) vGlut1+ and (**E**) vGlut2+ puncta / µm^2 and (**F**) the ratio of vGlut1+ to vGlut2+ in nucleus reuniens in developing *Xkr8*-WT and *Xkr8*-cKO mice thalamus. All data shown as mean ± SEM, scatter plot represents individual animals, n = 5-6. Mixed model ANOVA, LSM *post-hoc* test, ***p<0.001, **p<0.01, *p<0.05.

3.3   Conditional *Xkr8* knock out does not affect developmental cortical loss

Emx1::Cre driver used in our conditional knock out mouse line was expressed from embryonic day 10 (E10, Iwasato *et al.*, 2004), therefore it was active during cortical neurogenesis, which includes postnatal cortical cell loss. To confirm that increased density of vGlut1+ synapses in developing cortex (Figure 12) was not due to the decreased developmental neuronal loss, we evaluated number of cells, thickness of the cortex and the density of cells in primary somatosensory cortex and layer IV (L4) in early and juvenile *Xkr8*-WT and *Xkr8*-cKO mice (Figure 12).

We observed no significant differences in the number of primary somatosensory cortex cells and cortical thickness in P8 and P28 *Xkr8*-WT mice (Figure 12A-D). The total density of DAPI-stained cells significantly decreased during development in *Xkr8*-WT mice ($p<0.001$, Figure 12G). This showed that the total number of cells in the primary somatosensory cortex and cortical thickness of the cortex was stable in P8 and P28 *Xkr8*-WT mice. We also evaluated the total number of cells in the L4 of the primary somatosensory cortex and observed no significant differences when comparing P8 and P28 *Xkr8*-WT mice (Figure 12A-B, E). Although cortical thickness did not change, we observed a significant increase in L4 thickness in P28 *Xkr8*-WT mice (Figure 12A-B, F).

Even though *Emx1*::Cre driver was expressed from E10 and therefore Xkr8 would have been lost from pyramidal neurons in *Xkr8*-cKO mice during postnatal cortical cell loss, we did not observe any significant differences in either total cortical cell number and density or layer IV cell number and density between early postnatal *Xkr8*-WT and *Xkr8*-cKO mice (Figure 12A-H). This shows that cortical cell loss was not impaired in *Xkr8*-cKO mice and occurred in the same manner as in *Xkr8*-WT mice during brain development.
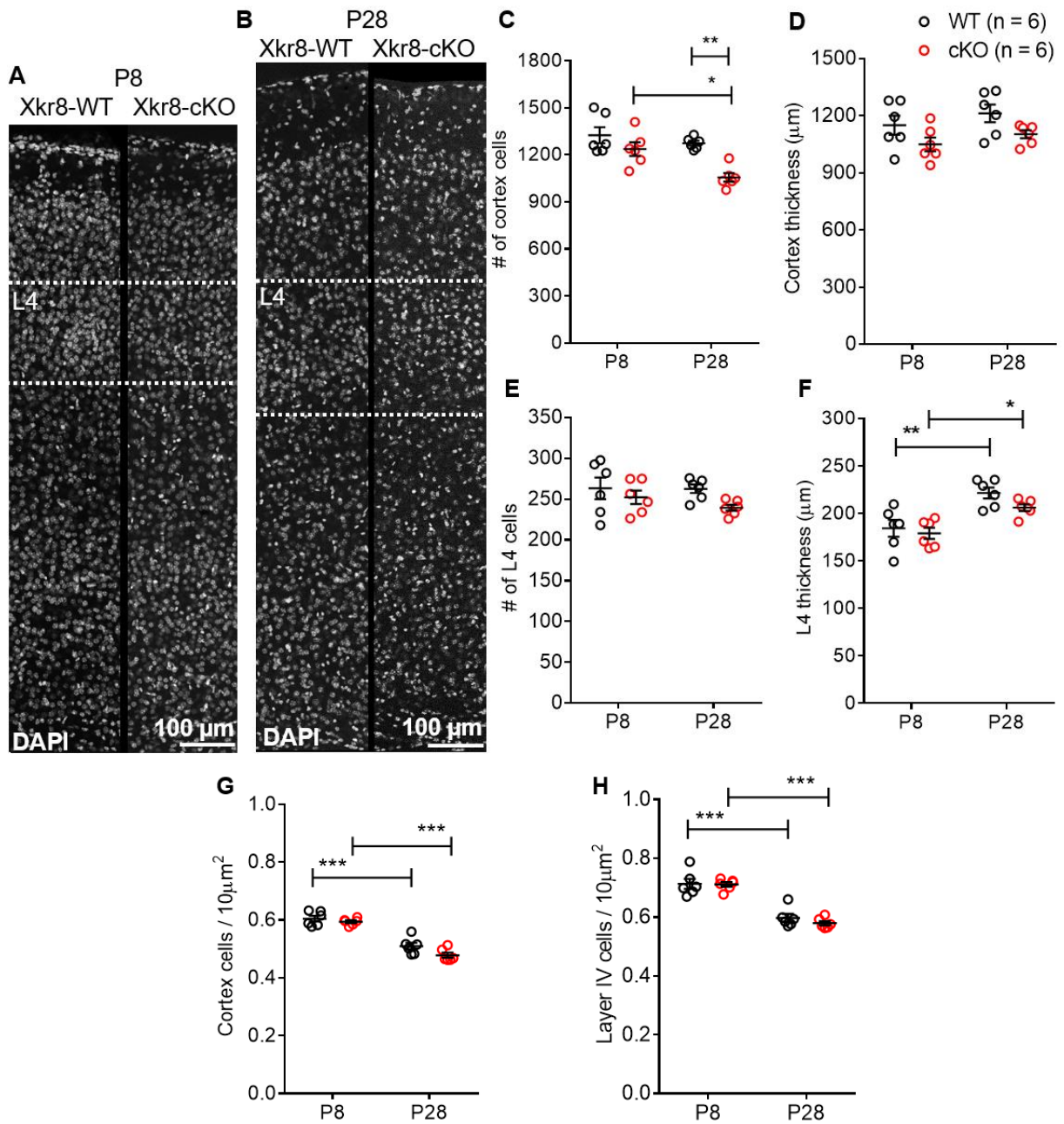
Figure 12. Cell density in primary somatosensory cortex in *Xkr8*-WT and *Xkr8*-cKO mice. Representative images of DAPI-stained nuclei in (**A**) P8 *Xkr8*-WT, P8 *Xkr8*-cKO and (**B**) P28 *Xkr8*-WT, P28 *Xkr8*-cKO layer IV (L4, white dashed arrow) and primary somatosensory cortex (scale bar 100 µm). The number of cells in (**C**) primary somatosensory cortex and (**E**) layer IV / µm^2 in developing *Xkr8*-WT and *Xkr8*-cKO mice. The thickness of (**D**) primary somatosensory cortex and (**F**) layer IV (µm) in developing *Xkr8*-WT and *Xkr8*-cKO mice. The density of cells in (**G**) primary somatosensory cortex and (**H**) layer IV / 10µm^2 in developing *Xkr8*-WT and *Xkr8*-cKO mice. All data shown as mean ± SEM, scatter plot represents individual animals, n = 6. Mixed model ANOVA, LSM *post-hoc* test, *p<0.05, **p<0.01, ***p<0.001.

3.4   The effect of disrupted PtdSer scrambling on corticospinal axonal pruning

One of the well characterised systems of axonal pruning is the development of corticospinal tracts projecting from cortical layer V (L5) neurons. To assess the density of corticospinal axons in wild-type mice and those lacking Xkr8 in pyramidal neurons, we used a modified Palmgren silver staining described by Goshgarian (1977) to visualise corticospinal axons in medulla sections in P8 *Xkr8*-WT and *Xkr8*-cKO mice (Figure 13).

We observed a significant increase ($p<0.001$) in total axon count in randomly selected bundles in corticospinal tract area while comparing P8 *Xkr8*-WT and *Xkr8*-cKO mice (Figure 13A-G). This showed that Xkr8 scramblase was required in cortical axon pruning during early brain development and further confirmed that PtdSer acted as an "eat-me" signal during brain development.
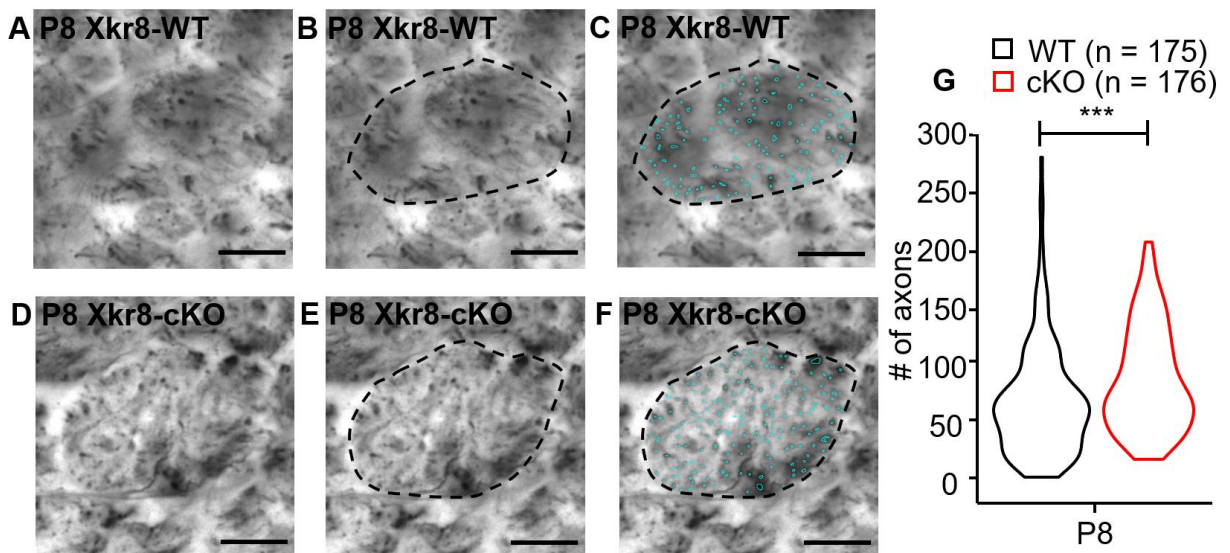
Figure 13. Corticospinal axons visualised by modified Palmgren silver staining (Goshgarian, 1977) in P8 *Xkr8*-WT and *Xkr8*-cKO mice. Representative images of silver-stained corticospinal tract area in medulla sections in (**A-C**) P8 *Xkr8*-WT and (**D-F**) P8 *Xkr8*-cKO mice (scale bar 10 µm). (**B**) and (**E**) Bundle area (dashed line) in (**A**) and (**D**), respectively (scale bar 10 µm). (**C**) and (**F**) Axon outlines (cyan) in the bundle area of (**A**) and (**D**), respectively (scale bar 10 µm). (**G**) The number of axons in randomly selected bundles in corticospinal tract area in *Xkr8*-WT and *Xkr8*-cKO mice. The violin plot outlines illustrate distribution of the data. Mann-Whitney test, ***$p<0.001$.

4. DISCUSSION

In this study, we investigated the role of phospholipid scramblase Xkr8 in synaptic pruning during brain development. First of all, we confirmed that Xkr8 scramblase is expressed in the neocortex of *Xkr8*-WT mice. Further experiments involved transgenic conditional Xkr8 scramblase knock-out mice line, in which *Xkr8* was selectively knocked out from neocortical neurons expressing *Emx1*. Successful elimination of *Xkr8* from pyramidal neurons was validated by immunohistochemical staining, demonstrating the lack of Xkr8-specific signal in the neocortex of *Xkr8*-cKO mice.

Conditional Xkr8 knock-out from cortical excitatory neurons allowed us to compare cortical connections with impaired PtdSer scrambling with non-affected thalamic connections. Our results indicated that synaptic pruning of cortico-cortical connections, that lacked Xkr8-dependent PtdSer exposure, was impaired and resulted in three-fold increase in the number of cortical connections, whereas thalamo-cortical connections were pruned normally. This showed, that altered PtdSer scrambling in presynaptic compartment impaired synaptic pruning, whereas postsynaptic PtdSer was not sufficient to trigger and/or mediate synaptic pruning.

We eliminated Xkr8 scramblase using Cre-loxP system. It is known that *Emx1*::Cre driver is expressed from E10 onwards. This coincides with major cortical development events, including cortical cell loss. Therefore, we assessed cortical cell density in P8 *Xkr8*-WT, *Xkr8*-cKO and P28 *Xkr8*-WT, *Xkr8*-cKO mice. We did not observe any differences when comparing *Xkr8*-WT with *Xkr8*-cKO mice. Here we showed that cortical cell loss was not impaired in *Xkr8*-cKO mice and occurred in the same manner as in *Xkr8*-WT mice during brain development. Thus the increase of presynaptic structure density was not due to higher cell number but was likely a result of impaired synaptic pruning.

Finally, we evaluated cortical axonal pruning under normal and impaired *Xkr8* scramblase expression and observed a significant increase of axons in corticospinal tract area in P8 *Xkr8*-cKO mice. This once again confirmed that Xkr8-dependent PtdSer-scrambling was required in cortical axonal pruning during early brain development.

To validate the role of microglia in PtdSer-dependent synaptic pruning, there is still a need to perform a phagocytosis assay directly evaluating the effect of disrupted Xkr8 expression on axonal material engulfment by microglia.

Our findings complement few recent experiments. Electrophysiological study carried out by D. Ragozzino group at Sapienza University (Rome, Italy) showed that adult *Xkr8*-cKO mice maintain immature circuits characterised by higher mean spontaneous excitatory postsynaptic current peak amplitude, lower trend of evoked excitatory postsynaptic current peak amplitude, higher paired-pulse ration and lower AMPA/NMDA ratio. In addition, recent resting state functional magnetic resonance imaging study carried out by A. Gozzi group at Center for Neuroscience and Cognitive Systems at Italian Institute of Technology (Rovereto, Italy), which demonstrated that *Xkr8*-cKO animals displayed a major increase in global interhemispheric connectivity. Future experiments must inevitably include behaviour experiments to validate molecular findings described in our study. Since our results show global brain network impairments, *Xkr8*-WT and *Xkr8*-cKO mice could demonstrate social abnormalities, motor dysfunctions and learning and memory deficits.

CONCLUSIONS

Altogether our data demonstrated that:

- Xkr8 scramblase is expressed in the neocortex in *Xkr8*-WT mice and is eliminated from the pyramidal neurons in *Xkr8*-cKO mice.
- Presynaptic PtdSer exposure is required for normal synaptic pruning in somatosensory cortex.
- The increase of presynaptic structure density in *Xkr8*-cKO mice is not due to lower developmental loss of cortical neurons, but is likely a result of impaired synaptic pruning.
- Disruption of PtdSer scrambling interferes with developmental elimination of corticospinal axons.

VILNIUS UNIVERSITY

LIFE SCIENCES CENTER

Kristina Jevdokimenko

Master thesis

THE ROLE OF THE PHOSPHOLIPID SCRAMBLASE XKR8 IN THE DEVELOPING
BRAIN

SUMMARY

During synaptic pruning synapses are eliminated from neuronal network. This process needs to be strictly controlled, since under-pruning and over-pruning are associated with physiological and morphological impairments, leading to various neurodevelopmental diseases, such as autism spectrum disorder or schizophrenia. Nowadays the amount of validated experiments is increasingly showing that during brain development synaptic pruning is mediated by brain macrophages – microglia. One of the molecular cues in microglia-neuron interaction is an "eat-me" signal phosphatidylserine (PtdSer).

In this study, we investigated the role of PtdSer scramblase XK-related protein 8 (Xkr8) in brain development. To understand how PtdSer exposure contributes to microglia-mediated synaptic pruning we investigated a transgenic $Xkr8^{Flx/Flx}$; $Emx1$::Cre; $Thy1$::GFP mouse line ($Xkr8$-cKO) with impaired Xkr8 expression in Emx1 excitatory neurons. We were interested whether insufficient PtdSer exposure on Xkr8-lacking neurons will affect the elimination of the synapses of these neurons during brain development. For this reason, we investigated two sets of connections differing in PtdSer exposure: cortico-cortical and thalamo-cortical connections and vice versa. It is known that $Emx1$::Cre driver is expressed in $Xkr8$-cKO mice line and is active during postnatal cortical cell loss. Therefore, we investigated whether ablation of Xkr8 scramblase in excitatory neocortical neurons affected their development. Finally, we used a well described corticospinal tract system to evaluate cortical axonal pruning under normal and impaired Xkr8 scramblase expression.

Our data demonstrated that Xkr8 scramblase is expressed in the neocortex in $Xkr8$-WT mice and is eliminated from the pyramidal neurons in $Xkr8$-cKO mice. Moreover, presynaptic PtdSer exposure is required for normal synaptic pruning. Finally, disruption of PtdSer scrambling interferes with developmental elimination of corticospinal axons.

VILNIAUS UNIVERSITETAS

GYVYBĖS MOKSLŲ CENTRAS

Kristina Jevdokimenko

Magistrinis darbas

FOSFOLIPIDŲ SKRAMBLAZĖS XKR8 VAIDMUO BESIVYSTANČIOSE SMEGENYSE

SANTRAUKA

Sinapsių šalinimas iš neuronų tinklo – sinapsių genėjimas – turi būti tinkamai reguliuojamas, kadangi nepakankams ar perteklinis sinapsių genėjimas yra siejamas su fiziologiniais ir morfologiniais sutrikimais, galinčiais sukelti įvairias neurovystymosi ligas, tokias kaip autizmo spektro sutrikimą ir šizofreniją. Pastaraisiais metais vis daugėja duomenų, kad sinapsių genėjimą kontroliuoja mikroglijos ląstelės. Viena iš molekulių mikroglijos-neuronų sąveikoje yra "valgyk mane" signalas fosfatidilserinas (PtdSer).

Šiame darbe buvo tiriama PtdSer skramblazės su XK-susijusio baltymo 8 (Xkr8) vaidmuo besivystančiose smegenyse. Norint suprasti, kaip PtdSer ekspozicija susijusi su nuo mikroglijos priklausomu sinapsių genėjimu buvo tiriama genetiškai modifikuota $Xkr8^{Flx/Flx}$; $Emx1$::Cre; $Thy1$::GFP pelių linija ($Xkr8$-cKO), kurioje buvo sutrikdyta Xkr8 raiška Emx1 sužadinamuosiuose neuronuose. Buvo tiriama ar nepakankama PtdSer ekspozicija ant Xkr8 neturinčių neuronų paviršiaus paveiks šių neuronų sinapsių šalinimą vystymosi metu. Buvo nagrinėjamos dvi poros jungčių, besiskiriančių PtdSer ekspozicija. Žievėje buvo vertinamos vidužievinės ir gumburą su žieve jungiančios jungtys. Gumbure buvo vertinamos vidugumburinės ir žievę su gumburu jungiančios jungtys. Yra žinoma, kad $Emx1$::Cre yra reiškiamas naudojamoje $Xkr8$-cKO pelių linijoje ir yra aktyvus žievės vystymosi metu, kai vyksta žievės ląstelių žūtis. Dėl šios priežasties buvo tiriama ar Xkr8 skramblazės sutrikdymas darė įtaką sužadinamųjų žievinių neuronų vystymuisi. Galiausiai naudojant žievinių nugaros smegenų laidų sistemą buvo įvertinta žievės aksonų genėjimas esant normaliai ir sutrikdytai Xkr8 skramblazės raiškai.

Šiame darbe buvo nustatyta Xkr8 skramblazės raiška Xkr8 laukinio tipo pelių žievėje ir patvirtinta, jog Xkr8 skramblazės raiška nevyksta $Xkr8$-cKO pelėse. Taip pat buvo nustatyta presinapsinės PtdSer ekspozicijos svarba normaliam sinapsių genėjimui. Galiausiai buvo patvirtinta, kad sutrikdyta PtdSer ekspozicija daro įtaką žievinių nugaros smegenų laidų genėjimui.

REFERENCES

1. Aloisi, F. (2001) 'Immune function of microglia', *Glia*, 36(2), pp. 165–179. doi: 10.1002/glia.1106.
2. Bagri, A. *et al.* (2003) 'Stereotyped Pruning of Long Hippocampal Axon Branches Triggered by Retraction Inducers of the Semaphorin Family', 113, pp. 285–299.
3. Brown, G. C. and Neher, J. J. (2014) 'Microglial phagocytosis of live neurons', *Nature Reviews Neuroscience*. Nature Publishing Group, 15(4), pp. 209–216. doi: 10.1038/nrn3710.
4. Carrillo, J., Nishiyama, N. and Nishiyama, H. (2013) 'Dendritic Translocation Establishes the Winner in Cerebellar Climbing Fiber Synapse Elimination', *Journal of Neuroscience*, 33(18), pp. 7641–7653. doi: 10.1523/JNEUROSCI.4561-12.2013.
5. Casano, A. M. and Peri, F. (2015) 'Microglia: Multitasking specialists of the brain', *Developmental Cell*. Elsevier Inc., 32(4), pp. 469–477. doi: 10.1016/j.devcel.2015.01.018.
6. Chung, W. S. *et al.* (2013) 'Astrocytes mediate synapse elimination through MEGF10 and MERTK pathways', *Nature*, 504(7480), pp. 394–400. doi: 10.1038/nature12776.
7. Feng, G. *et al.* (2000) 'Imaging neuronal sets in transgenic mice expressing multiple spectral variants of GFP', *Neuron*, 28(1), pp. 41–51.
8. Fremeau Jr, R. T. *et al.* (2004) 'VGLUTs define subsets of excitatory neurons and suggest novel roles for glutamate', *Trends in Neurosciences*, 27(2), pp. 98–103. doi: 10.1016/j.tins.2003.11.005.
9. Gardai, S. J. *et al.* (2005) 'Cell-surface calreticulin initiates clearance of viable or apoptotic cells through trans-activation of LRP on the phagocyte', *Cell*, 123(2), pp. 321–334. doi: 10.1016/j.cell.2005.08.032.
10. Glantz, L. A. and Lewis, D. A. (2000) 'Decreased Dendritic Spine Density on Prefrontal Cortical Pyramidal Neurons in Schizophrenia', *Archives of General Psychiatry*, 57, pp. 65–73.
11. Goshgarian, H. G. (1977) 'A Rapid Silver Impregnation Nerve Fibers in Paraffin NOTE for Central and Peripheral and Frozen Sections', 301, pp. 296–301.
12. Harris, K. D. and Mrsic-flogel, T. D. (2013) 'Cortical connectivity and sensory coding', *Nature*. Nature Publishing Group, 503(7474), pp. 51–58. doi: 10.1038/nature12654.
13. Hashimoto, K. and Kano, M. (2013) 'Synapse elimination in the developing cerebellum', *Cellular and Molecular Life Sciences*, 70(24), pp. 4667–4680. doi: 10.1007/s00018-013-1405-2.
14. Holers, V. M. (2014) 'Complement and Its Receptors: New Insights into Human Disease', *Annual Review of Immunology*, 32(1), pp. 433–459. doi: 10.1146/annurev-immunol-032713-120154.
15. Innocenti, G. M. and Price, D. J. (2005) 'EXUBERANCE IN THE DEVELOPMENT OF CORTICAL NETWORKS', 6(December), pp. 955–965. doi: 10.1038/nrn1790.
16. Iwasato, T. *et al.* (2000) 'Cortex-restricted disruption of NMDAR1 impairs neuronal patterns in the barrel cortex', *Nature*, 406(6797), pp. 726–731. doi: 10.1038/35021059.
17. Iwasato, T. *et al.* (2004) 'Dorsal Telencephalon-Specific Expression of Cre Recombinase in PAC Transgenic Mice', *Genesis*, 38(3), pp. 130–138. doi: 10.1002/gene.20009.
18. Kemshead, J. T. *et al.* (1982) 'Human Thy-1: expression on the cell surface of neuronal and glial cells.', *Brain research*, 236, pp. 451–461.
19. Kristóf, E. *et al.* (2013) 'Novel role of ICAM3 and LFA-1 in the clearance of apoptotic neutrophils by human macrophages', *Apoptosis*, 18(10), pp. 1235–1251. doi: 10.1007/s10495-013-0873-z.
20. Liang, K. J. *et al.* (2009) 'Regulation of dynamic behavior of retinal microglia by

CX3CR1 signaling', *Investigative Ophthalmology and Visual Science*, 50(9), pp. 4444–4451. doi: 10.1167/iovs.08-3357.

21. Mizutani, M. *et al.* (2012) 'The Fractalkine Receptor but Not CCR2 Is Present on Microglia from Embryonic Development throughout Adulthood', *The Journal of Immunology*, 188(1), pp. 29–36. doi: 10.4049/jimmunol.1100421.

22. Nagata, S. *et al.* (2016) 'Exposure of phosphatidylserine on the cell surface', *Cell Death and Differentiation*. Nature Publishing Group, 23(6), pp. 952–961. doi: 10.1038/cdd.2016.7.

23. Neniskyte, U. and Brown, G. C. (2013) 'Lactadherin/MFG-E8 is essential for microglia-mediated neuronal loss and phagoptosis induced by amyloid β', *Journal of Neurochemistry*, 126(3), pp. 312–317. doi: 10.1111/jnc.12288.

24. Nimmerjahn, A., Kirchhoff, F. and Helmchen, F. (2005) 'Neuroscience: Resting microglial cells are highly dynamic surveillants of brain parenchyma in vivo', *Science*, 308(5726), pp. 1314–1318. doi: 10.1126/science.1110647.

25. Ogden, C. A. *et al.* (2001) 'C1q and Mannose Binding Lectin Engagement of Cell Surface Calreticulin and Cd91 Initiates Macropinocytosis and Uptake of Apoptotic Cells', *The Journal of Experimental Medicine*, 194(6), pp. 781–796. doi: 10.1084/jem.194.6.781.

26. Paolicelli, R. C. *et al.* (2011) 'Synaptic Pruning by Microglia Is Necessary for Normal Brain Development', *Science*, 333, pp. 1456–1459.

27. Presumey, J., Bialas, A. R. and Carroll, M. C. (2017) *Complement System in Neural Synapse Elimination in Development and Disease*. 1st edn, *Advances in Immunology*. 1st edn. Elsevier Inc. doi: 10.1016/bs.ai.2017.06.004.

28. Redcay, E. and Courchesne, E. (2005) 'When is the brain enlarged in autism? A meta-analysis of all brain size reports', *Biological Psychiatry*, 58(1), pp. 1–9. doi: 10.1016/j.biopsych.2005.03.026.

29. Sacco, R., Gabriele, S. and Persico, A. M. (2015) 'Head circumference and brain size in autism spectrum disorder: A systematic review and meta-analysis', *Psychiatry Research - Neuroimaging*. Elsevier, 234(2), pp. 239–251. doi: 10.1016/j.pscychresns.2015.08.016.

30. Sapar, M. L. *et al.* (2018) 'Phosphatidylserine Externalization Results from and Causes Neurite Degeneration in Drosophila', *Cell Reports*. ElsevierCompany., 24(9), pp. 2273–2286. doi: 10.1016/j.celrep.2018.07.095.

31. Schafer, D. P. *et al.* (2012) 'Microglia Sculpt Postnatal Neural Circuits in an Activity and Complement-Dependent Manner', *Neuron*. Elsevier Inc., 74(4), pp. 691–705. doi: 10.1016/j.neuron.2012.03.026.

32. Segawa, K. and Nagata, S. (2015) 'An Apoptotic "Eat Me" Signal: Phosphatidylserine Exposure', *Trends in Cell Biology*. Elsevier Ltd, 25(11), pp. 639–650. doi: 10.1016/j.tcb.2015.08.003.

33. Selemon, L. D. and Zecevic, N. (2015) 'Schizophrenia: A tale of two critical periods for prefrontal cortical development', *Translational Psychiatry*. Nature Publishing Group, 5(8), pp. e623-11. doi: 10.1038/tp.2015.115.

34. Smith, I. W. *et al.* (2013) 'Terminal Schwann Cells Participate in the Competition Underlying Neuromuscular Synapse Elimination', *Journal of Neuroscience*, 33(45), pp. 17724–17736. doi: 10.1523/JNEUROSCI.3339-13.2013.

35. Sozzani, S. *et al.* (1996) 'Chemokines: A superfamily of chemotactic cytokines', *International Journal of Clinical and Laboratory Research*, 26(2), pp. 69–82. doi: 10.1007/BF02592349.

36. Stephan, A. H., Barres, B. A. and Stevens, B. (2012) 'The Complement System: An Unexpected Role in Synaptic Pruning During Development and Disease', *Annual Review of Neuroscience*, 35(1), pp. 369–389. doi: 10.1146/annurev-neuro-061010-113810.

37. Stevens, B. *et al.* (2007) 'The Classical Complement Cascade Mediates CNS Synapse Elimination', *Cell*, 131, pp. 1164–1178. doi: 10.1016/j.cell.2007.10.036.

38. Suzuki, J. *et al.* (2013) 'Xk-related protein 8 and CED-8 promote phosphatidylserine exposure in apoptotic cells', *Science*, 341(6144), pp. 403–406. doi: 10.1126/science.1236758.

39. Suzuki, J., Imanishi, E. and Nagata, S. (2014) 'Exposure of phosphatidylserine by Xk-related protein family members during apoptosis', *Journal of Biological Chemistry*, 289(44), pp. 30257–30267. doi: 10.1074/jbc.M114.583419.

40. Suzuki, J., Imanishi, E. and Nagata, S. (2016) 'Xkr8 phospholipid scrambling complex in apoptotic phosphatidylserine exposure', *Proceedings of the National Academy of Sciences*, 113(34), pp. 9509–9514. doi: 10.1073/pnas.1610403113.

41. Suzuki, K. *et al.* (2013) 'Microglial Activation in Young Adults With Autism Spectrum Disorder', *JAMA Psychiatry*, 70(1), p. 49. doi: 10.1001/jamapsychiatry.2013.272.

42. Tang, G. *et al.* (2014) 'Article Loss of mTOR-Dependent Macroautophagy Causes Autistic-like Synaptic Pruning Deficits', *Neuron*. Elsevier Inc., 83, pp. 1131–1143. doi: 10.1016/j.neuron.2014.07.040.

43. Vadišiūtė, A. (2017) *The role of Xkr8 scramblase in microglia-dependent synaptic pruning: morphological and electrophysiological study*. Vilnius University.

44. Vanderhaeghen, P. and Cheng, H.-J. (2009) 'Guidance Molecules in Axon Pruning and Cell Death', *Cold Spring Harbor Perspectives in Biology*, (2), pp. 1–18.

45. Wyatt, S. K. *et al.* (2017) 'Enhanced classical complement pathway activation and altered phagocytosis signaling molecules in human epilepsy', *Experimental Neurology*. Elsevier Inc., 295, pp. 184–193. doi: 10.1016/j.expneurol.2017.06.009.

46. Zhan, Y. *et al.* (2014) 'Deficient neuron-microglia signaling results in impaired functional brain connectivity and social behavior', *Nature Neuroscience*. Nature Publishing Group, 17(3), pp. 400–406. doi: 10.1038/nn.3641.

SUPPLEMENTARY INFORMATION

One of the most widely used resource of protein expression in the brain is Allen Brain Atlas. However, this tool lacks *in situ* hybridization data for Xkr8 scramblase in developing mouse brain. Using *in situ* hybridization we confirmed the expression of Xkr8 in the neocortex in *Xkr8*-WT mice (Supplementary Fig. 1). Our data shows that Xkr8 is specifically expressed in the granular cell layer of hippocampus and cortex (Supplementary Fig. 1A-B, mXkr8 anti-sense probe). There was little to no expression in hindbrain region (Supplementary Fig. 1C). Using mXkr8 exon 3 sense probe as a negative control we observed no signal in any of the regions (Supplementary Fig. 1, mXkr8 exon 3 sense probe). This confirms that Xkr8 scramblase is predominantly expressed in the developing neocortex.
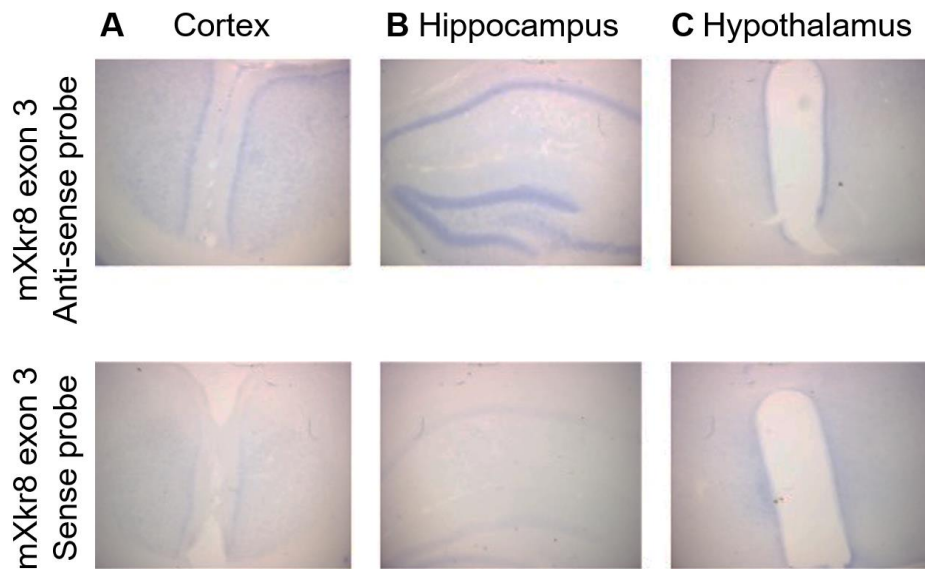
Supplementary Figure 1. Use of RNAscope to visualise Xkr8 exon 3 gene expression in *Xkr8*-WT mice. Qualitative images of Xkr8 signal (blue to dark magenta) in P8 *Xkr8*-WT (**A**) cortex, (**B**) hippocampus and (**C**) hypothalamus using mXkr8 exon 3 anti-sense and sense probe.

In situ hybridization data for Xkr8 scramblase expression in mouse brain was obtained by Dr. Emerald Perlas at the European Molecular Biology Laboratory, Italy.